Identifying Contributing Factors of Occupant Thermal Discomfort in a Smart Building

Aniruddha Basak[1], **Ole Mengshoel**[1], **Stefan Hosein**[2], **Rodney Martin**[3], **Jayasudha Jayakumaran**[1], **Mario Gurrola Morga**[4], and **Ishwari Aghav**[1]
Carnegie Mellon University Silicon Valley[1], University of the West Indies, St. Augustine[2],
NASA Ames Research Center[3], Zapopan's Superior Institute of Technology[4]
abasak@cmu.edu, ole.mengshoel@sv.cmu.edu, stefan.hosein2@my.uwi.edu,
rodney.martin@nasa.gov, jayasudha.jayakumaran@sv.cmu.edu,
mariogurrolam@gmail.com, ishwari.aghav@sv.cmu.edu

Abstract

Modeling occupant behavior in smart buildings to reduce energy usage in a more accurate fashion has garnered much recent attention in the literature. Predicting occupant comfort in buildings is a related and challenging problem. In some smart buildings, such as NASA AMES Sustainability Base, there are discrepancies between occupants' actual thermal discomfort and sensors based upon a weighted average of wet bulb, dry bulb, and mean radiant temperature intended to characterize thermal comfort. In this paper we attempt to find other contributing factors to occupant discomfort. For our experiment we use a dataset from a Building Automation System (BAS) in NASA Sustainability Base. We choose one conference room for our experiment and empirically establish the thermal discomfort level for the room's temperature sensor. We use various causality metrics and causal graphs to isolate candidate causes of the target room temperature. And we compare these feature sets according to their predictive capability of future instances of discomfort. Moreover, we establish a trade off between computational and statistical performance of adverse event prediction.

Introduction

Predicting building energy consumption and designing adaptive schemes for energy savings have been a well-discussed topic in the literature (Kolter and Ferreira Jr 2011; Hamdy, Hasan, and Siren 2011; Oldewurtel et al. 2012). Various techniques based on model predictive control have shown to improve building energy efficiency (Širokỳ et al. 2011). However, different occupant behavior can lead to large disagreement between measured and predicted energy usage in buildings with same function (Hong 2014). Therefore occupant behavior modeling in smart buildings has attracted many researchers (Baptista et al. 2014; Dong and Andrews 2009).

Despite recent developments in occupant behavior modeling, predicting occupant comfort (or discomfort) in building environment is a challenging problem (Dobbs and Hencey 2014; Federspiel, Bridges, and Langkilde 1998; Federspiel 2001). Fanger's model (Fanger and others 1970) , being the most widely accepted thermal comfort model, has been adopted as part of ASHRAE (American Society of Heating, Refrigerating, and Air-Conditioning Engineers) 55 standard. However, determining thermal comfort by Fanger's double heat balance equations has its limitations. One example is the impacts of thermal radiation field on thermal comfort (Halawa, van Hoof, and Soebarto 2014). In practice there are discrepancies between occupants' actual thermal discomfort and sensors based upon a weighted average of wet bulb, dry bulb, and mean radiant temperature intended to characterize thermal comfort (Federspiel, Martin, and Yan 2004).

Figure 1: An aerial photograph of SB building.

A similar scenario occurred in NASA Ames Sustainability Base[1] (SB), a green building that provides a research testbed for different sustainable technologies and concepts. The SB (aerial view[2] in Figure 1) is designed with a Net Zero Energy objective. One major area of consumption is the building heating and cooling system. Detailed monitoring of the BAS is required at regular intervals. SB is instrumented with 2636 sensors, which perform physical or logical measurements. From Nov 2014 to May 2015 many "cold complaints" were issued by the occupants. A cold complaint can originate from an anomalous drop in building temperature or unexpected cool environment in conference rooms in the morning.

An essential step to eliminating these complaints is to

[1] http://www.nasa.gov/ames/facilities/sustainabilitybase

[2] http://www.nasa.gov/centers/ames/multimedia/images/2012/iotw/sustainability-base-aerial.html

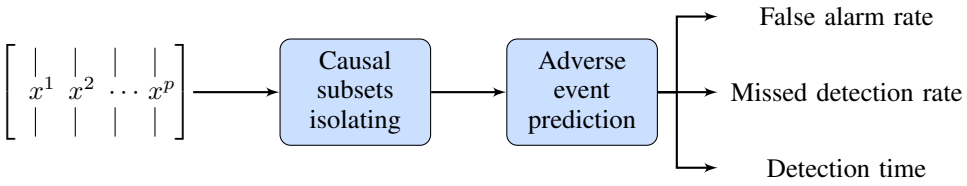

Figure 2: Data processing steps

identify the contributing factors to occupant discomfort. In this work we use a few causal discovery methods to solve this problem in a data driven approach. First, we established an empirical threshold of a conference-room's temperature for representing the associated cold complaints. We call this room temperature sensor, the "target variable" (x^*). Next we used the sensor data collected from the BAS of the SB building to learn causal subsets relevant to that temperature sensor. Autoregressive model, Granger causality test and causal graphs were used as learning models in the experiments.

The causal subsets were then fed to an adverse event prediction toolbox, ACCEPT (Adverse Condition and Critical Event Prediction Toolbox) (Martin et al. 2015), which provides a single, unifying framework for comparative performance assessment of results from the application of a variety of algorithmic methods. ACCEPT produces results in the form of missed detection (false negative), false alarm (false positive) rate and detection time (the number of time steps in advance the system can predict an anomalous event), which are essential in generating our results.

Related Research

A comprehensive overview of many methods to evaluate and predict occupant thermal comfort is presented in (Olesen 2004; Federspiel, Bridges, and Langkilde 1998). Lately, various machine learning techniques have been applied to model thermal comfort. Different human body factors (blood volume pressure, skin temperature, respiration rate and skin conductance) and environmental measurements (e.g ambient temperature, humidity, air motion and so forth) have been used to prediction occupant comfort levels using correlations and Predictive Mean Vote (PMV) model (Burzo et al.). The impact of climate, glazing type, and shading properties on thermal comfort in an office environment has been studied in (Bessoudo et al. 2010).

Identifying the more suitable set of features among environmental, psychological and physiological attributes, to predict thermal comfort level, have also been attempted (Farhan et al. 2015). The authors compared Support Vector Machine (SVM) and Random Forest classifiers with Fanger's model and found that the accuracy of SVM classifier was two times higher than Fanger's model. Kernel methods have also been applied for thermal comfort forecasting. Locally weighted regression has been shown to provide more accurate prediction than PMV in (Manna, Wilson, and Brown 2013). To the best of our knowledge, causal learning algorithms have not been used to identify the contributing factors to thermal comfort.

Procedure

The data processing components of our analysis is shown in Figure 2. Using multiple causal learning techniques we isolated subsets of features from time series data collected from the BAS. These feature subsets are used for adverse event prediction. The performance metrics of prediction are false alarm rate (false positive rate), missed detection rate (false negative rate) and the detection time (the number of timesteps in advance a warning is generated).

In this section we describe the casual isolation methods and adverse event prediction technique.

Causal subsets isolation

- **Granger Causality test**, a hypothesis test promoted by the econometrician Clive Granger (Granger 1969), helps in determining whether the past values of one time series can be leveraged in predicting the future values of another. Hence, this test can be directly used to identify features with causal relationship with the target (x^*).

  This causality test is based on a series of F-tests where each test determines if a feature has statistically significant information about the future values of x^*. The test statistic has a F-distribution under the null hypothesis.

  For each variable x^i, the null and alternative hypothesis for the test are as follows

  $$H_0 : x^i \text{ does not Granger cause } x^*$$
  $$H_1 : x^i \text{ Granger causes } x^*.$$

  The linear model according to H_1 is called unrestricted (UR) regression model. And the model without x^i, as per H_0, serves as the restricted (R) regression model. The parameters of these models are learned form the training data. If the sum of squared residuals of the trained R and UR models are SSR_R and $SSR_U R$ respectively, the test statistic (F) is defined as follows,

  $$F = \frac{(SSR_R - SSR_{UR})/p}{(SSR_{UR})/(N-p-1)} \quad (1)$$

  where N is the number of observations in training data and p is the number of variables.

  If the value of F is greater than the critical value of F-distribution, the null hypothesis is rejected. This critical value is dependent on the significance level (α) of the test. If the null hypothesis is rejected for x^i, it is considered to Granger cause x^*.

- **Autoregressive (AR) models** are often used in economics and for modeling time-varying natural processes (Kelejian and Prucha 2010; Chakraborty et al. 2012). We used an autoregressive model of order τ, AR(τ), to express the target as a linear combination of all time-lagged variables,

$$y_t^{(j)} = \mathbf{a}_1^T \mathbf{y}_{t-1} + \mathbf{a}_2^T \mathbf{y}_{t-2} + \cdots + \mathbf{a}_\tau^T \mathbf{y}_{t-\tau} + e_t^{(j)} \quad (2)$$
$$= \beta^T \mathbf{Y}_{t-1,t-\tau} + e_t^{(j)}$$

where $y_t^{(j)} = x^*$ is the target, $\mathbf{y}_t \in \mathbb{R}^p$ is a vector containing the values of all variables at time t and a_t is the corresponding weight vector. $\mathbf{Y}_{t-1,t-\tau} \in \mathbb{R}^{p\tau}$ and $\beta \in \mathbb{R}^{p\tau}$ concatenates the variables and weights respectively. To reduce non-informative variables we train the model with a sparsity constraint. Our optimization formulation is as follows,

$$\hat{\beta}_L = \underset{\beta \in \mathbb{R}^{p\tau}}{\arg\min} \sum_{t=\tau}^{T} \left(y_t^{(j)} - Y_{t-1,t-\tau}\beta\right)^2 + \lambda ||\beta||_L \quad (3)$$

where the regularization norm, L, is chosen to 2. We select the first k variables, sorted in decreasing order of the weights in the trained model $\hat{\beta}_L$, as *informative variables*.

- **Causal graph learning** We use two causal graph structure learning algorithms: PC and GES. Both are widely used methods and theoretically correct.

PC (Spirtes and Glymour, Social Science Computer Review, 1991) is a pattern search algorithm for which the input is an acyclic causal structure. The input dataset should be either entirely continuous or entirely discrete. When the input dataset is continuous, the causal relation between any two variables is linear and the distribution for each variable is Normal. The PC algorithm sometimes outputs double-headed edges on a large sample limit. This indicates that the adjacent variables have an unrecorded common cause. PC algorithm constructs the graph structure based on conditional independence relations in the data. For continuous datasets, PC algorithm uses tests of zero correlation or zero partial correlation for independence or conditional independence respectively.

The GES algorithm is a stable greedy equivalency search algorithm that runs under the same input assumptions as the PC algorithm but the output patterns are always the same. The GES is a score based algorithm. It scores all possible orientations of edges between variables, and higher the score, the better the approximation should be. The penalty discount, the parameter given to the GES algorithm affects which edges are discarded. The higher the penalty discount the more robust an edge must be to remain the output graph. One variation of the GES algorithm is the iMAGES algorithm which runs the GES algorithm on all datasets multiple times, with increasing penalty discounts, until there are no three-variable cliques left in the graph.

Adverse Event Prediction

Adverse event prediction is the process of identifying potential adverse events in a system before they occur. This is necessary for situations where an adverse event can be problematic or fatal. By selecting informative features, prediction can occur within a reasonable time horizon of an actual adverse event so that mitigating action can be taken to stop the adverse event from occurring. Hence, we use the ACCEPT (Adverse Condition and Critical Event Prediction) Toolbox (Martin et al. 2015) to perform this prediction.

In ACCEPT, all data is preprocessed and filtered. In Fig. 3, the regression toolbox contains multiple regression techniques as support vector regression (SVR), k-nearest neighbor regression (k-NN), linear regression (LR), bagged neural nets (BNN), extreme learning machines (ELM), etc. We use LR and ELM in our experiments. ELM is similar to a single layer feed-forward neural network with one difference that the input layer parameters are assigned randomly.

ACCEPT employs an unsupervised machine learning approach for its architecture, meaning that no labeled data is used to supervise the process of model learning. As such, all training data associated with the regression step is by definition nominal data. Anomalous data is reserved solely for validation and testing purposes, and does not influence the model characterized by the regression step described above. In this way, two distinct classes of machine learning algorithms, regression and classification, are employed within ACCEPT. Classification methods based upon hypothesis tests are used to determine if any novel, anomalous data is out of family with respect to the regression model characterizing the nominal training data.

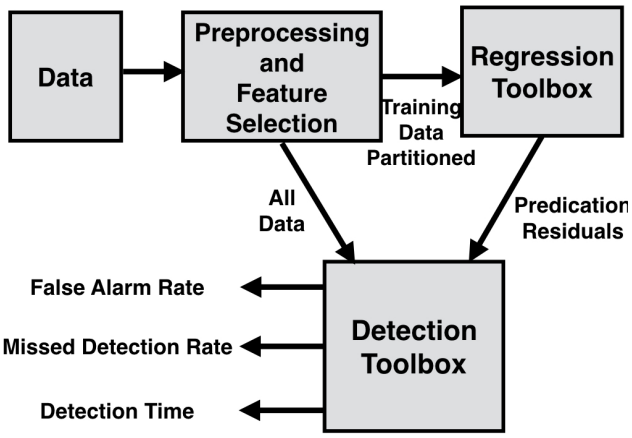

Figure 3: Architecture of ACCEPT.

The results of ACCEPT contain the false alarm rate, the missed detection rate and the detection time. Here, the detection time is defined as the number of timesteps in advance a warning is generated. By utilizing these metrics we can compare the different causal learning techniques.

Experiments and Results

Data and Methods

Our data set consists 26,493 samples (Nov 2014 to Feb 2015) from 2,636 sensors of the BAS of NASA SB building.

Type of Sensor	Number of sensors
Temperature	273
Current	191
Valve	201
Set point	267
Others	581

Table 1: Feature categories in the NASA SB dataset

These sensors measure various physical and logical quantities (such as room temperature, humidity, pressure in flow pipes, status of heat pump, etc) and record in 5 minutes interval. A brief categorical description of the features is presented in Table 1.

As a preprocessing step of our experiments, we centered and scaled every sensor data to make the mean 0 and variance 1. We used 60% of total samples for training models, 10% for validation and 30% for testing.

While training autoregressive model, we observed that strong correlations exist among room-temperature sensors measurements. As temperature in different rooms is controlled by a central heating-cooling system, similar variations exist in multiple room-temperature sensors. Thus for proper causal discovery, we removed all temperature sensors, except the target, from the dataset.

In the first set of experiments we isolate the causal subsets using the previously described methods. A summary of all subsets is presented in Table 2. Next we establish an empirical comfort threshold for the target variable. Finally we use ACCEPT to compare the predictability of the causal subsets in forecasting adverse events of the target variable.

Causal subsets isolation

- **GC test** Using significance level $\alpha = 0.005$, we perform the F-tests for every feature in the dataset. We construct a causal subset by including all features in GC_{test} for which the null hypothesis was rejected.

  Moreover, we sort the features in GC_{test} according to their deviation from the critical value of F-test and choose the top features as candidate causes. The subset with top k features is denoted as GC^k_{test}.

- **Autoregressive model training** First, we train an AR(1) model with x^* as output and all sensors in the dataset as inputs. Due to rank deficiency of the training data matrix, we add a small ridge penalty (λ) on the parameters. We compare this model with an AR(1) model trained with tuned λ. The tuning is performed in a separate validation set.

  Figure shows the predictions of these two models. Clearly, the trained model with tuned λ shows superior performance than the small λ counterpart. We use the model parameters of the tuned to select *informative variables* from the dataset. As all features are in the same scale (part of pre-processing), we select k informative variables as the top k features, sorted in descending order of the parameter values. The denote this set as $C^k_{AR+\text{ridge}}$.

- **Causal graph learning** We use PC and GES algorithms to learn causal graph over the variables in the dataset. As the computation time of structure learning with large number of features is very high (Figure 8), we attempted to learn causal variables with all features and a subset of informative variables. For the first case, we denote the identified causes as $C^{\text{full}}_{\text{PC/GES}}$. And the causes identified from a graph learned over k informative variables are denoted by $C^k_{\text{PC/GES}}$.

  For the PC algorithm, we used Gaussian conditional independence test with significance level $\alpha = 0.01$. And the score function for GES algorithm was Bayesian Information Criterion (BIC). We found that the graph structure changes significantly with increasing number of features fed to the structure learning algorithm. Thus the set of identified causes does not always grow with increasing features, i.e

$$C^{k_1}_{\text{PC}} \nsubseteq C^{k_2}_{\text{PC}} \nsubseteq C^{\text{full}}_{\text{PC}} \text{ for any } k_1 < k_2 < p. \qquad (4)$$

Empirical discomfort threshold

An empirical approach was taken to determine the ground truth for the *cold complaints* prediction scenario. We estimated the distribution of the target room temperature sensor (x^*) and found that it was a unimodal distribution with mean 71.7 and standard deviation 1.8. Hence, a 95% confidence interval around the mean corresponds to 68.1°F and 75.3°F. Considering this range as nominal room temperature values, we established 68.1°F as the upper threshold for cold regions. In our problem, we are only concerned with anomalous drops in temperature. Thus, we considered any temperature value below 68.1°F as an *adverse event* (cold). And there are multiple adverse events as shown in Figure 4.

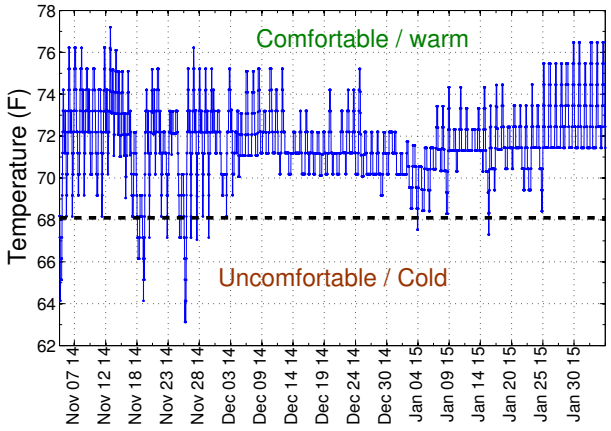

Figure 4: Cold and warm temperature regions according to empirical analysis.

Comparison using ACCEPT

The goal of this experiment is to compare the performance of causal subsets in predicting adverse events of the target

Feature Set (F)	Number of features $\|F\|$	Identification method
GC^5_{test}, GC^{10}_{test}, GC^{20}_{test}	5, 10, 20	Granger causality test
$C^5_{AR+\text{ridge}}$, $C^{10}_{AR+\text{ridge}}$, $C^{20}_{AR+\text{ridge}}$, $C^{100}_{AR+\text{ridge}}$	5, 10, 20, 100	AR model with ridge penalty
C^5_{GES} , C^{10}_{GES} C^{20}_{GES}	3, 1, 6	GES algorithm
C^5_{PC}, C^{10}_{PC} , C^{20}_{PC}	3, 1, 6	PC algorithm
C^{100}_{PC} , $C^{p/2}_{\text{PC}}$, $C^{\text{full}}_{\text{PC}}$	6, 7, 6	

Table 2: Descriptions of all feature set

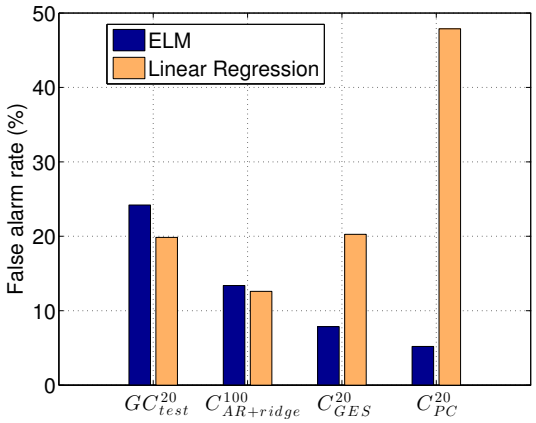

(a) Comparison of false alarm rates.

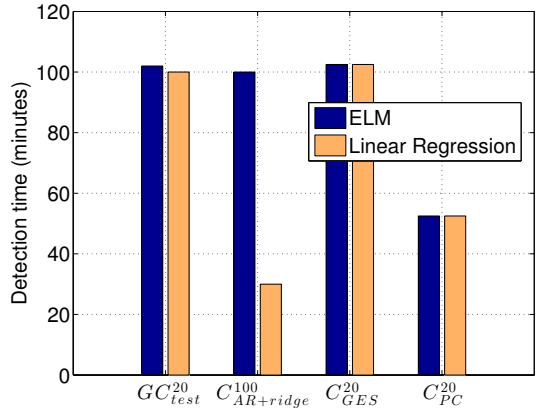

(b) Comparison of detection times.

Figure 5: Comparison of Extreme Learning Machine (ELM) and Linear Regression (LR) models.

based on the derived empirical threshold. As ACCEPT is

Feature Set	False Alarm Rate (%)	Missed Detection Rate (%)	Detection Time (minutes)
GC^5_{test}	24.20	0.00	102.50
GC^{10}_{test}	24.20	0.00	102.50
GC^{20}_{test}	24.20	0.00	102.50
$C^5_{AR+\text{ridge}}$	22.00	0.00	97.50
$C^{10}_{AR+\text{ridge}}$	21.00	0.00	97.50
$C^{20}_{AR+\text{ridge}}$	21.55	0.00	97.50
$C^{100}_{AR+\text{ridge}}$	13.38	1.90	100.00
C^5_{GES}	25.27	0.00	102.50
C^{10}_{GES}	2.44	0.48	100.00
C^{20}_{GES}	7.86	0.00	102.50
C^5_{PC}	8.28	0.00	52.50
C^{10}_{PC}	8.28	0.00	52.50
C^{20}_{PC}	**5.20**	**0.00**	**52.50**
C^{100}_{PC}	14.54	0.95	97.50
$C^{p/2}_{\text{PC}}$	23.25	0.00	100.00
$C^{\text{full}}_{\text{PC}}$	23.14	0.00	100.00

Table 3: Results for all causal subsets

designed to train models only using continuous features, the discrete features are discarded from each causal subset.

First we compare the linear regression (LR) and extreme learning machine (ELM) models, as part of ACCEPT's regression toolbox, in terms of false alarm rates and detection times. Missed detection rates are very small in all cases and thus omitted. Figure 5 shows the comparison prediction results for one feature set from each identification method. We observe that in all cases, ELM model performs similar or better than LR model. Hence, for the next experiments we exclusively use ELM model for regression in ACCEPT.

Table 3 shows the results for all causal subsets produced by ACCEPT. There is no subset which achieves minimum false alarm and missed detection rates which maximizing the detection time. To comprehend the results we first compare the subsets form each identification method separately. Then we make inter-method comparison.

Figure 6 shows results of AR model features with increasing feature set sizes. We see an inverse relation between false alarm rate and detection time. Moreover, with small increase in detection time $C^{100}_{AR+\text{ridge}}$ achieves significant decrease in false alarm rate. Hence we can conclude that the causal subsets (of AR model) with higher size have superior predictability of adverse events.

There is no change in prediction performance of $GC^{|F|}_{\text{test}}$ subsets with increasing size (Table 3). However $C^{|F|}_{AR+\text{ridge}}$

achieves lower false alarm rate than $GC^{|F|}_{\text{test}}$ with approximately similar detection time. Hence the AR model in superior to Granger causality test for this problem.

Small variation in the false alarm rates is seen for C^k_{GES} subsets. In contrast significant variations in all three metrics can be observed for C^k_{PC} features. Figure 7 compares the performance of these causal subsets. The best trade-off between the three metrics is accomplished by C^{20}_{PC}.

Although C^k_{PC} subsets do not grow monotonically with increasing k, we observed that there are one or many overlapping features among all subsets. This indicate high significance of these overlapping features in affecting thermal discomfort.

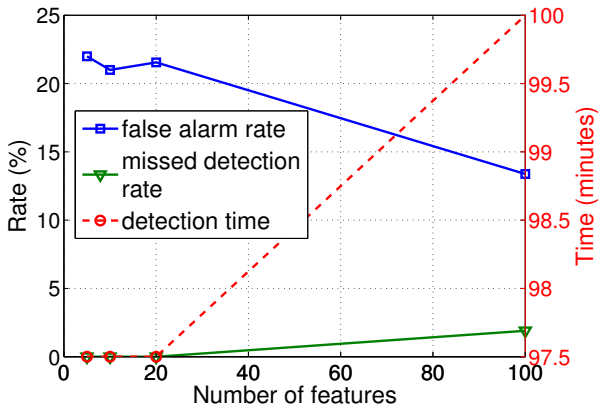

Figure 6: Comparison of ACCEPT results for $C^{|F|}_{AR+\text{ridge}}$ features.

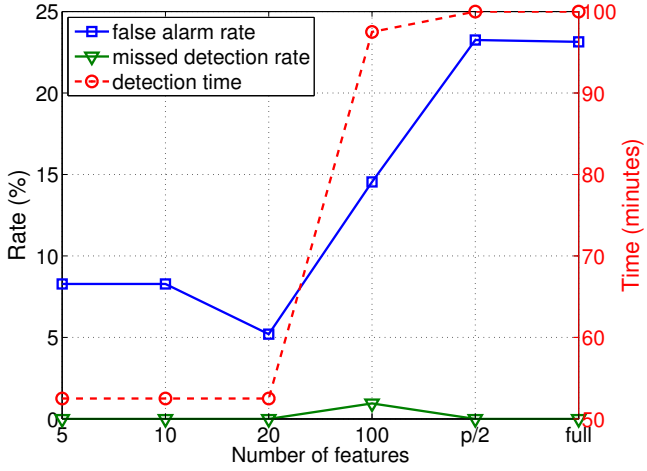

Figure 7: Comparison of ACCEPT results for causal features identified by the PC algorithm.

Trade-off between computational and statistical performance

We observed that the training time in ACCEPT increases non-linearly with increasing number of features. In the previous comparison we observed superior performance from causal subsets identified by AR model and the PC algorithm. Also we seen large feature sets are required for low false alarm rate by AR model subsets. Here the computational cost of adverse event prediction using these subsets is dominated by ACCEPT's run-time.

On the contrary, causal subsets isolated by the PC algorithm do not grow with increasing features in the dataset. Thus the computational cost, in this case, is dominated by PC run-time. Figure 8 compares the run-times of causal subset identification and adverse event prediction combined, for increasing feature set sizes. In both ACCEPT performs prediction. We observe that both grow super-linearly. However the run-time of "AR + ACCEPT" is a few-order magnitude higher than the "PC + ACCEPT". Although AR model's causal features exhibit more stable statistical performance, they demand much higher computational time. Thus we can conclude that a good trade-off between computational and statistical performance can be achieved using the PC algorithm.

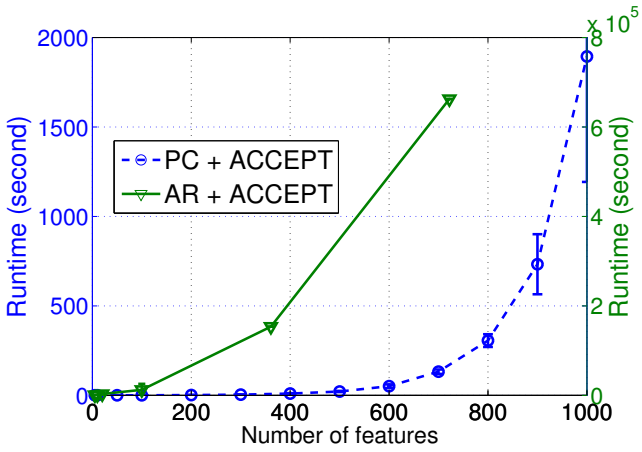

Figure 8: Runtime comparison of causal subset identification (PC and AR) and adverse event prediction combined, with increasing number of features.

Conclusion and Future Work

In this work we presented an alternate approach for identifying contributing factors of occupant discomfort. We used various causal learning method to isolate candidate causes associated with a target room-temperature. Empirically, we established the discomfort level for a conference room and used the candidate causes to predict cold temperatures in the room. We found that the candidate causes identified by autoregressive model and the PC algorithm explained the adverse events well. However, good trade off between computation time and prediction accuracy was achieved by the PC algorithm. Thus we recommend causal graph learning approach for occupant discomfort modeling.

Future work will be directed towards using the discomfort model to design energy efficient schemes for maintaining occupant comfort in smart buildings.

References

Baptista, M.; Fang, A.; Prendinger, H.; Prada, R.; and Yamaguchi, Y. 2014. Accurate household occupant behavior modeling based on data mining techniques. In *Proceedings of the Twenty-Eighth AAAI Conference on Artificial Intelligence*, 1164–1170.

Bessoudo, M.; Tzempelikos, A.; Athienitis, A.; and Zmeureanu, R. 2010. Indoor thermal environmental conditions near glazed facades with shading devices–part i: Experiments and building thermal model. *Building and Environment* 45(11):2506–2516.

Burzo, M.; Wicaksono, C.; Abouelenien, M.; Pérez-Rosas, V.; Mihalcea, R.; and Tao, Y. Multimodal sensing of thermal discomfort for adaptive energy saving in buildings.

Chakraborty, P.; Marwah, M.; Arlitt, M. F.; and Ramakrishnan, N. 2012. Fine-grained photovoltaic output prediction using a bayesian ensemble. In *AAAI Conference on Artificial Intelligence*.

Dobbs, J. R., and Hencey, B. M. 2014. Model predictive hvac control with online occupancy model. *Energy and Buildings* 82:675–684.

Dong, B., and Andrews, B. 2009. Sensor-based occupancy behavioral pattern recognition for energy and comfort management in intelligent buildings. In *Proceedings of building simulation*, 1444–1451.

Fanger, P. O., et al. 1970. Thermal comfort. analysis and applications in environmental engineering. *Thermal comfort. Analysis and applications in environmental engineering.*

Farhan, A. A.; Pattipati, K.; Wang, B.; and Luh, P. 2015. Predicting individual thermal comfort using machine learning algorithms. In *Automation Science and Engineering (CASE), 2015 IEEE International Conference on*, 708–713. IEEE.

Federspiel, C. C.; Bridges, B.; and Langkilde, G. 1998. Statistical analysis of unsolicited thermal sensation complaints in commercial buildings/discussion. *ASHRAE Transactions* 104:912.

Federspiel, C. C.; Martin, R. A.; and Yan, H. 2004. Recalibration of the complaint prediction model. *HVAC&R Research* 10(2):179–200.

Federspiel, C. 2001. Estimating the frequency and cost of responding to building complaints in: Spengler, j. sammet j. and mccarthy, j. eds. *Indoor Air Quality Handbook, McGraw Hill*.

Granger, C. W. 1969. Investigating causal relations by econometric models and cross-spectral methods. *Econometrica: Journal of the Econometric Society* 424–438.

Halawa, E.; van Hoof, J.; and Soebarto, V. 2014. The impacts of the thermal radiation field on thermal comfort, energy consumption and controla critical overview. *Renewable and Sustainable Energy Reviews* 37:907–918.

Hamdy, M.; Hasan, A.; and Siren, K. 2011. Impact of adaptive thermal comfort criteria on building energy use and cooling equipment size using a multi-objective optimization scheme. *Energy and Buildings* 43(9):2055–2067.

Hong, T. 2014. Occupant behavior: impact on energy use of private offices. In *ASim 2012-1st Asia conference of International Building Performance Simulation Association., Shanghai, China, 11/25/12-11/27/12*.

Kelejian, H. H., and Prucha, I. R. 2010. Specification and estimation of spatial autoregressive models with autoregressive and heteroskedastic disturbances. *Journal of Econometrics* 157(1):53–67.

Kolter, J. Z., and Ferreira Jr, J. 2011. A large-scale study on predicting and contextualizing building energy usage.

Manna, C.; Wilson, N.; and Brown, K. N. 2013. Personalized thermal comfort forecasting for smart buildings via locally weighted regression with adaptive bandwidth. In *SMARTGREENS*, 32–40.

Martin, R.; Das, S.; Janakiraman, V.; and Hosein, S. 2015. ACCEPT: Introduction of the adverse condition and critical event prediction toolbox. Technical Report NASA/TM-2015-218927, National Aeronautics and Space Administration (NASA).

Oldewurtel, F.; Parisio, A.; Jones, C. N.; Gyalistras, D.; Gwerder, M.; Stauch, V.; Lehmann, B.; and Morari, M. 2012. Use of model predictive control and weather forecasts for energy efficient building climate control. *Energy and Buildings* 45:15–27.

Olesen, B. W. 2004. International standards for the indoor environment. *Indoor Air* 14(s7):18–26.

Širokỳ, J.; Oldewurtel, F.; Cigler, J.; and Prívara, S. 2011. Experimental analysis of model predictive control for an energy efficient building heating system. *Applied Energy* 88(9):3079–3087.